



Providing Choice & Value

Generic CT and MRI Contrast Agents



CONTACT REP

AJNR

Morphometric Evaluation of the Facial and Vestibulocochlear Nerves Using MR Imaging in Patients with Menière Disease

Wilhelm H. Flatz, Annika Henneberger-Kunz, Regina Schinner, Ullrich Müller-Lisse, Maximilian Reiser and Birgit Ertl-Wagner

This information is current as of July 30, 2025.

AJNR Am J Neuroradiol published online 15 October 2024
<http://www.ajnr.org/content/early/2025/03/27/ajnr.A8537>

Morphometric Evaluation of the Facial and Vestibulocochlear Nerves Using MR Imaging in Patients with Menière Disease

Wilhelm H. Flatz,  Annika Henneberger-Kunz, Regina Schinner, Ullrich Müller-Lisse, Maximilian Reiser, and  Birgit Ertl-Wagner



ABSTRACT

BACKGROUND AND PURPOSE: Menière disease (MD) is a condition of unknown etiology, involving genetic predisposition, autoimmune processes, viral infections, cellular apoptosis, and oxidative stress. This study aimed to investigate potential differences in cranial nerves VII and VIII in patients with MD using hydrops MRI (FLAIR) for morphometric evaluations.

MATERIALS AND METHODS: Sequences acquired were 3T MRI, CISS, and 3D FLAIR. We evaluated the morphometrics of cranial nerves VII and VIII from the cerebellopontine angle to the internal auditory canal fundus, comparing the nonaffected and affected sides. Furthermore, we examined the findings in relation to symptom duration and evaluated the feasibility of FLAIR in the morphometry of the cranial nerves.

RESULTS: A total of 53 patients with MD with unilateral symptoms were included. After statistical analysis, no significant differences were found regarding morphometric changes in the affected side compared with the nonaffected side of cranial nerves VII and VIII. There was also no significant difference between the morphometric evaluations of patients with different symptom durations. The morphometric evaluation using hydrops MRI sequences (FLAIR) showed no significant difference compared with established morphometric highly T2-weighted imaging (CISS).

CONCLUSIONS: Our data found no differences in nerve morphometry between clinically nonaffected and affected sides in patients with unilateral MD, nor any correlation with symptom duration. This finding contrasts with previous ones of correlations between clinical features and endolymphatic hydrops. A disease process starting before clinical symptom onset could be a possible explanation. Morphometric evaluation of brain nerves using hydrops MRI sequences is practical and provides similar results compared with T2-weighted imaging, improving patient comfort and reducing MRI scan times.

ABBREVIATIONS: CN = cochlear nerve; CPA = cerebellopontine angle; CSA = cross-sectional area; FN = facial nerve; IAC = internal auditory canal; IVN = inferior vestibular nerve; LD = long diameter; MD = Menière disease; SD = short diameter; SVN = superior vestibular nerve

Menière disease (MD) is characterized by episodic vertigo associated with tinnitus, fluctuating hearing loss, aural fullness, and endolymphatic hydrops, but the exact pathomechanism of this condition remains unclear.^{1,2} It appears to be multifactorial or a complex cascade of pathophysiologic processes.^{3,4} Several studies proposed a loss of neural structures (such as hair cells or neurons within the spiral ganglion) in MD, whereas genetic causes, autoimmune processes, and viral or other infections have also been discussed.⁵⁻¹¹ In recent years, several studies have evaluated

and quantified endolymphatic hydrops in patients with MD.¹²⁻¹⁸ Only a few studies, however, have analyzed the morphometric parameters of cranial nerves VII and VIII on MRI, mostly in normal-hearing subjects or patients with sensorineural hearing loss or in children with hypoplasia or aplasia of the cochlear nerve in the context of cochlear implant diagnostics.¹⁹⁻²³

To our knowledge, there has been limited research on patients with MD regarding the cranial nerves. Although cellular death and apoptosis would theoretically lead to a decreased nerve thickness, previous data showed a swelling of cranial nerves VII and VIII in patients with MD compared with a normal-hearing control group.²² The swelling of cranial nerve VIII and the similar reaction of the facial nerve (FN) support, for example, mediator-based or systemic theories of MD pathophysiology. These theories suggest that small, circulating immune complexes could be deposited in tissues, leading to local inflammatory reactions through complement fixation.²⁴ These immune complexes could

Received April 5, 2024; accepted after revision October 8.

From the Department of Radiology (W.H.F., R.S., U.M.-L., M.R.), University Hospital, Ludwig Maximilian University Munich, Munich, Germany; HNOeins (A.H.-K.), Augsburg, Germany; and The Hospital for Sick Children (B.E.-W.), Toronto, Ontario, Canada.

Please address correspondence to Wilhelm H. Flatz, University Hospital, Department of Radiology, Marchioninistrasse 15, 81377 Munich, Germany; e-mail: wilhelm.flatz@med.uni-muenchen.de

 Indicates article with supplemental data.

<http://dx.doi.org/10.3174/ajnr.A8537>

SUMMARY

PREVIOUS LITERATURE: The pathogenesis of MD is still incompletely understood. Local processes such as excitotoxicity and reactive oxygen species leading to cellular apoptosis were discussed as well as genetic and autoimmune causes for systemic processes. For example, Kariya et al⁶ found a lower number of spiral ganglion cells in the contralateral temporal bone of patients with unilateral MD compared with healthy controls. Different FLAIR sequences were used in several studies to evaluate the endolymphatic hydrops. Several CISS sequences were used to analyze the morphometric properties of cranial nerves VII and VIII, mostly in normal-hearing patients or in patients with sensorineural hearing loss.

KEY FINDINGS: No differences of the morphometric parameters could be found comparing the nonaffected side with the affected side of unilaterally-affected patients with MD as well as comparing the subgroups with different durations of illness. Furthermore, FLAIR sequences can be similarly used compared with the established CISS sequences.

KNOWLEDGE ADVANCEMENT: Our results support systemic processes causing MD. Although each of the MR sequences examined showed different means for the morphometric parameters, each of the sequences was suitable for this purpose. Thus, after one acquires a good FLAIR sequence, the creation of a CISS for morphometric nerve analysis can be ignored.

lead to increased vascular permeability with subsequent ion and fluid imbalances.

The course of cranial nerves VII and VIII from the pons through the cerebellopontine angle (CPA) and the internal auditory canal (IAC) makes these nerves amenable to morphometric evaluation in anatomic and MRI studies. Cranial nerve VIII divides within the IAC into its 3 branches: cochlear nerve (CN), superior vestibular nerve (SVN), and inferior vestibular nerve (IVN). By default, these cranial nerves are evaluated using strongly T2-weighted sequences, eg, CISS sequences, while the imaging of endolymphatic hydrops is performed using FLAIR sequences, also called hydrops MRI. These hydrops MRI sequences have been shown to be of high value in the MR evaluation of the degree of endolymphatic hydrops in the structures of the inner ear.^{12,17,18,25,26} The value of the FLAIR hydrops MRI sequences regarding morphometric changes of the cranial nerves have not been evaluated yet. To our knowledge, no morphometric analyses of cranial nerves VII and VIII have been performed using different MRI sequences with different spatial resolutions in patients with clinically unilateral MD.

The aim of this study was to investigate morphometric differences of the cranial nerves VII and VIII in patients with MD using different MR imaging techniques to find further clues to the underlying pathogenesis. Additionally, the second objective of our study was to streamline the requirement for various MRI sequences used in evaluating endolymphatic hydrops and cranial nerve morphometry, aiming to decrease scan duration and enhance patient comfort.

MATERIALS AND METHODS

Participants

Ethics review board approval was provided by the institutional review board (Ludwig Maximilian University Munich). All examinations were performed in accordance with the Helsinki Declaration revised in 2013.

Seventy-one patients from our database had definite MD according to the American Academy of Otolaryngology–Head and Neck Surgery classification in 1995 and the latest 2015 modification of the diagnostic criteria of the Bárány Society Classification

Committee.^{14,28–31} Figure 1 shows the 2015 proposed criteria of MD. Of these 71 patients, 53 patients were clinically and audiometrically classified as unilaterally affected (20 women, 33 men; mean age, 50.5 years; age range, 23–77 years) and were therefore included in this study.

Additional clinical patient data were collected to calculate symptom duration, which ranged from 4 to 252 months, with a mean of 76 months.

MR Imaging

All patients gave their informed consent for MRI of the inner ear. Twenty-four hours before the MRI scan a gadolinium-based contrast agent diluted 8-fold in saline solution was intratympanically injected into the ear of the affected side.^{25,32} After administration, the patient remained in a supine position for another 30 minutes with the head turned approximately 45° toward the contralateral side.

All MR imaging examinations were performed on a 3T MR unit (Magnetom Verio; Siemens) using a commercially available 4-channel flexible surface coil combined with an 8-channel head coil. To determine if measurements of the cranial nerves VII and VIII produce results comparable at different slice thicknesses, we varied the slice thickness in the MR sequences used. The following MR sequences were acquired of the temporal bone:

- CISS 0.6: A strongly T2-weighted CISS, which is a 3D steady-state sequence with free precession with the following parameters: TR = 7.2 ms, TE = 3.16 ms, flip angle = 70°, field of view = 192 × 192 mm², matrix size = 320 × 320, averages = 1, and slice thickness = 0.6 mm
- CISS 0.4: The second CISS sequence had the following parameters: TR = 6.24 ms, TE = 2.87 ms, flip angle = 70°, field of view = 160 × 160 mm², matrix size = 320 × 320, averages = 1, and slice thickness = 0.4 mm
- FLAIR 0.5: The 3D TSE sequence with inversion recovery precession (FLAIR) was acquired using the following parameters: TR = 6000 ms, TE = 155 ms, TI = 1500 ms, flip angle = 180°, field of view = 160 × 160 mm², matrix size = 320 × 320, averages = 1, and slice thickness = 0.5 mm
- FLAIR 0.3: The second inversion recovery sequence had the following parameters: TR = 6000 ms, TE = 155 ms, TI = 1500 ms,

Menière disease criteria proposed 2015

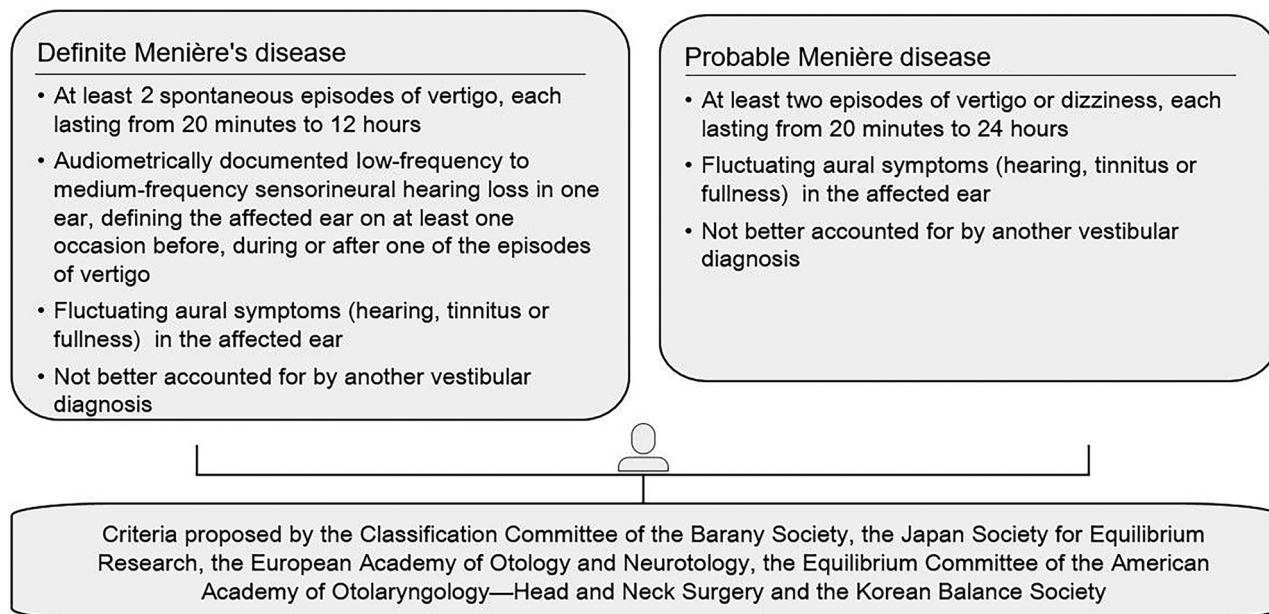


FIG 1. MD criteria proposed in 2015 by the Classification Committee of the Barany Society.



FIG 2. IAC using CISS 0.6.

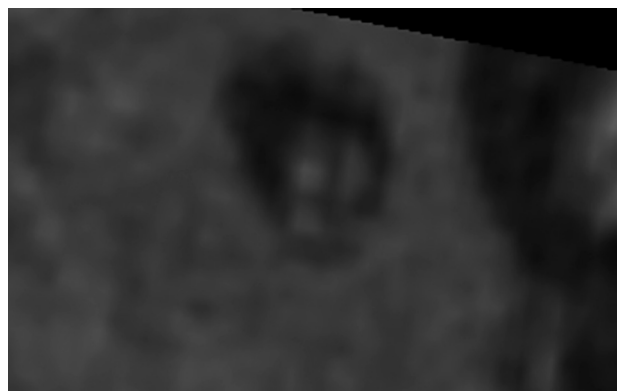


FIG 4. IAC using FLAIR 0.5.



FIG 3. IAC using CISS 0.4.

flip angle = 180°, field of view = 160 × 160 mm², matrix size = 256 × 256, averages = 1, and slice thickness = 0.3 mm.

Figures 2-5 show the IAC of 4 different patients in the sequences described above. Endolymphatic hydrops was assessed in the affected ear using the FLAIR sequences, capable of visualizing endolymphatic hydrops.^{12,14,31-37} In all patients, endolymphatic hydrops was confirmed using a 4-point Likert scale: Zero was no hydrops, and 1-3 was light, moderate, or severe hydrops.

Analysis

Morphometric analysis of cranial nerves VII and VIII was performed, retrospectively, on both sides, the locally enhanced inner ear side and the contralateral side. We used a commercial and freely available DICOM Viewer (OsiriX v.4.0, 64-bit version, <http://www.osirix-viewer.com>, and RadiAnt 2023.1, 64-bit version, Medixant) for measuring the diameters of cranial nerves VII and VIII. Consistent windowing levels and thin slice thicknesses

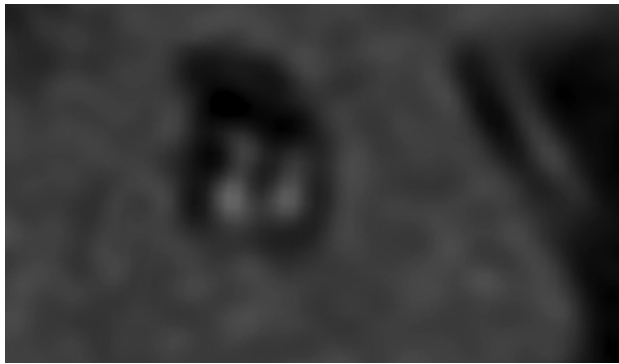


FIG 5. IAC using FLAIR 0.3.



FIG 8. The CSA of cranial nerve VIII in the CPA of the nonaffected side using FLAIR 0.5.

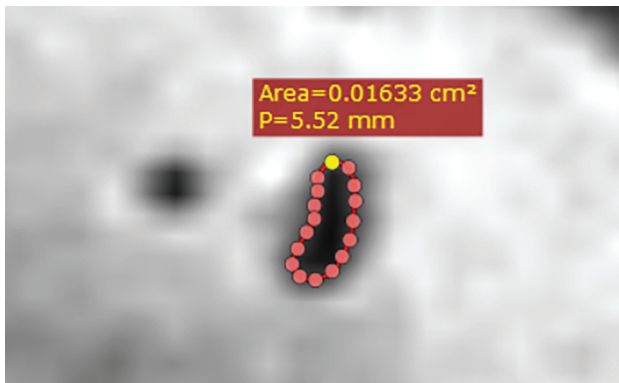


FIG 6. The CSA of cranial nerve VIII in the CPA of the affected side using CISS 0.4.



FIG 9. The CSA of cranial nerve VII in the CPA of the affected side using the FLAIR 0.3.

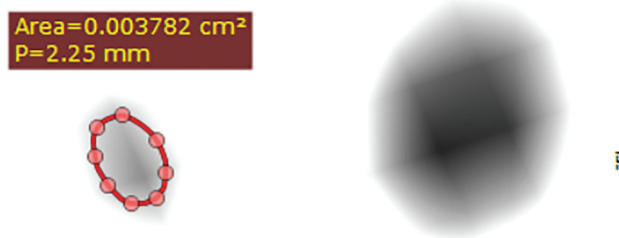


FIG 7. The CSA of cranial nerve VII in the CPA of the nonaffected side using CISS 0.6.

were used in performing transverse reformats at different locations throughout the course of the nerves from the CPA to the IAC fundus. Locations of the transverse sections were defined as follows:

- VIII, CPA
- CN, SVN, and IVN, meatus of the IAC
- VII, CPA, meatus of the IAC, fundus of the IAC.

On each transverse section, the long diameter (LD), short diameter (SD) perpendicular to LD, and cross-sectional area (CSA) were measured. Several dot markers were positioned on the outline of the examined nerves. These markers were linked, and the CSA was calculated. All measurements were performed by the same 2 readers on the basis of consensus readings (measurement time for the above 21 measurements per side and sequence of 13–

28 minutes). Both readers were blinded to the diagnoses of the patients. All these measurements were made for the CISS 0.4, CISS 0.6, and FLAIR 0.3 and the FLAIR 0.5 sequences to investigate different nerve sizes, depending on the MRI sequence used and the feasibility of morphometric analysis of cranial nerves VII and VIII in the endolymphatic hydrops sequences (FLAIR 0.3 and FLAIR 0.5) compared with the CISS standard sequences (Figs 6–9).

For comparing the affected and clinically nonaffected sides, a paired samples (dependent) *t* test was used with MedCalc Version 12.7.2 (MedCalc Software byba) and SAS Version 9.4 for Windows (SAS Institute). After Bonferroni correction for multiple testing, $P < .05$ was reduced to $P < .000595$ for statistical significance. To compare the subgroups of different symptom durations, we used a 2-sided independent samples *t* test. In addition, the 2 readers repeated the measurements independently (Table 1, eg, showing the CSA measurements of the affected side of cranial nerves VII and VIII in the CPA using CISS 0.4) to calculate an interrater and intrarater correlation for reproducibility (Spearman ρ for rank correlation).

RESULTS

No significant differences were observed when comparing the affected side with the nonaffected side of cranial nerves VII and VIII of clinically unilaterally-affected patients with MD

(Supplemental Data, CISS 0.4) when adjusting for multiple testing. These results were found to be independent of the MRI sequence used (CISS 0.4, CISS 0.6, FLAIR 0.5, or FLAIR 0.3) when adjusting for multiple testing (Table 2, cranial nerve VIII within CPA). Without the Bonferroni correction, to account for an exploratory approach, significant differences were found, for example, for the LD cranial nerve VII at the CPA and the fundus of the IAC as well as for the SD of cranial nerve VIII at the CPA using the CISS 0.4 (Supplemental Data) and the CSA of cranial nerve VIII in FLAIR 0.3 at the level of CPA (Table 2). Table 3 shows all the significant differences without the Bonferroni correction ($P < .05$), obviously not following a specific pattern.

We furthermore evaluated the morphometric properties of cranial nerves VII and VIII depending on symptom duration. We initially split the study group into a subgroup with a symptom duration of a maximum of 12 months and compared these patients with the rest of the group. We observed no significant differences between the groups, neither when comparing the affected sides nor when comparing the nonaffected sides. Subsequently, we compared patients with a symptom duration of at least 120 months with the patients with a symptom duration of a maximum of 12 months. Again, no significant differences for the morphometric parameters could be observed (Table 4).

Table 1: Measurements of the CSAs^a

Patient No.	CSA of VIII within CPA			CSA of VII within CPA		
	Consensus	Rater 1	Rater 2	Consensus	Rater 1	Rater 2
25	1.7	1.66	2.06	0.23	0.25	0.29
71	1.6	1.69	1.83	0.44	0.40	0.67
73	1.0	1.02	1.04	0.32	0.46	0.46
74	1.1	1.41	1.42	0.59	0.64	0.62
75	1.5	1.52	1.83	0.35	0.64	0.42
13	2.2	2.12	2.56	0.44	0.78	0.89
9	1.5	1.47	2.00	0.34	0.39	0.41
1	1.1	1.40	1.37	0.41	0.53	0.51
16	1.6	1.63	1.93	0.26	0.39	0.33
27	1.7	1.63	1.83	0.17	0.24	0.18
26	1.8	1.88	2.08	0.31	0.47	0.49
11	1.5	1.68	1.59	0.26	0.33	0.29
4	1.3	1.38	1.35	0.37	0.39	0.41
17	1.6	1.60	1.86	0.47	0.51	0.60
8	1.3	1.39	1.40	0.23	0.28	0.22
14	2.1	2.01	2.14	0.45	0.48	0.52

^aThe consensus reading results and the independently repeated measurements of raters 1 and 2 of the CSA (square millimeter) of the affected side of cranial nerves VIII and VII measured in the CPA using the CISS 0.4 sequence show a good inter- and intrarater correlation of the measurements.

Table 2: Comparison of the 4 used MRI sequences^a

Sequence		LD (mm)		SD (mm)		CSA (mm ²)	
		Nonaffected	Affected	Nonaffected	Affected	Nonaffected	Affected
CISS 0.4	Mean	1.81 (SD, 0.40)	1.81 (SD, 0.34)	0.86 (SD, 0.18)	0.78 (SD, 0.16)	1.68 (SD, 0.45)	1.58 (SD, 0.40)
	<i>P</i>		.9910		.0295 ^b		.0624
CISS 0.6	Mean	1.43 (SD, 0.24)	1.34 (SD, 0.24)	0.85 (SD, 0.17)	0.86 (SD, 0.16)	1.39 (SD, 0.30)	1.33 (SD, 0.31)
	<i>P</i>		.0857		.8386		.3886
FLAIR 0.3	Mean	1.71 (SD, 0.22)	1.57 (SD, 0.32)	0.92 (SD, 0.16)	0.89 (SD, 0.13)	1.72 (SD, 0.22)	1.57 (SD, 0.28)
	<i>P</i>		.0805		.4427		.0098 ^b
FLAIR 0.5	Mean	1.59 (SD, 0.28)	1.65 (SD, 0.22)	0.89 (SD, 0.15)	0.89 (SD, 0.20)	1.61 (SD, 0.31)	1.48 (SD, 0.23)
	<i>P</i>		.4575		.9187		.3051

^aThis table depicts the measurements of cranial nerve VIII within the CPA of clinically unilaterally-affected patients with MD, comparing the nonaffected side with the affected side by a paired samples *t* test (mean, *P*) and comparing the 2 CISS sequences and the 2 FLAIR sequences.

^bSignificant *P* values without adjustment for multiple testing.

Regarding the second aspect of our study, the 2 examiners were also able to visualize and evaluate the cranial nerves in the endolymphatic hydrops sequences FLAIR 0.3 and FLAIR 0.5 without any relevant differences compared with the CISS sequences. For evaluation of intrarater correlation, we performed the Spearman ρ , indicating a strong-to-very strong positive correlation among the measurements. The Spearman ρ median was 0.880 ($\rho = 0.710-0.994$, SD = 0.08191; 95% CI, 0.8289-0.9551). The interrater correlation was moderate to very strong with a Spearman ρ median of 0.8420 ($\rho = 0.6360-0.9260$, SD = 0.1046; 95% CI, 0.7039-0.9068).

DISCUSSION

In our study group, we observed no significant differences between the clinically nonaffected side and the clinically affected side of unilaterally-affected patients with MD independent of the MRI sequence used when using the Bonferroni correction for multiple testing.

Different Models of Ethio-pathogenesis

The pathogenesis of MD is still incompletely understood, and the disease can be difficult to diagnose in the early stages.^{2,30,38} Autoimmune processes and viral infections, such as latent

herpes simplex virus type 1, may cause vestibular neuritis and may play a role in the induction of MD.^{39,40} In addition, patients with MD frequently have accompanying allergies and allergy mediators such as immunoglobulin E that exacerbate MD symptoms. Deposits of immunoglobulin E in the vestibular end organs indicate the ability of the inner ear to participate in immune reactions.⁴¹ The involved immunologic mechanisms are still not clear, but approximately one-third of the MD cases may have an autoimmune origin.⁹ Cytokines and their involvement in immune-related processes may play a significant role in the etiology of MD, as is currently under discussion. Their roles in inflammation, autoimmune processes, potential disruption of endolymphatic fluid

homeostasis, and promotion of fibrosis are areas of particular interest.^{42,43}

Further pathophysiologic aspects have been discussed, such as genetic predisposition, excitotoxicity, chronic otitis media, ischemia, cellular apoptosis, and oxidative stress.^{8,9,44-46} Reactive oxygen species, specifically nitric oxide, regulate the cochlear blood flow and lead to the release of mitochondrial cytochrome c, which is an important mediator of the intrinsic pathway of apoptosis.^{46,47} The presence of hydrops may thus cause neuronal damage in the inner ear via a process of excitotoxicity.^{1,48} This neuronal damage could possibly affect cranial nerve VIII and potentially also the cranial nerve VII.

However, our data showed no noticeable differences in nerve diameters between the clinically unaffected and affected sides in patients with unilaterally-affected MD. This lack of difference may suggest a more systemic process that causes subclinical reactions in the contralateral ear, even in patients who appear clinically unilaterally affected by MD. Kariya et al⁶ found similar results when comparing the mean number of spiral ganglion cells, the mean loss of inner and outer hair cells, and the damage of the stria vascularis in patients with unilateral MD. They could not find any significant differences when comparing the affected and the nonaffected sides, whereas there was a significant loss of hair cells and spiral ganglion cells in the contralateral temporal

bones compared with healthy controls. This result may support autoimmune processes or genetic predispositions, whereas local processes such as excitotoxicity and reactive oxygen species seem less likely. Genetic research into MD has also been making great strides recently. Further research in ethnic and geographically-based studies of the human genome with the development of cell and animal models will help to understand the pathomechanism of MD, as will improvements in MRI technology.⁴⁹ New data, for example, show possible changes in the microstructure of cranial nerve VIII in patients with MD using DTI, indicating a new potential imaging biomarker for the diagnosis of MD.⁵⁰

Moreover, our data did not show a correlation to clinical symptom duration, which again may point to a very long-standing underlying process before the onset of clinical symptoms. On the other hand, our results could also indicate that there is no change of cranial nerves VII and VIII in MD. However, a previous study was able to show that patients with MD have thicker nerves compared with a healthy control group.²²

MRI Difficulties

Moreover, our data showed different means at the same measuring levels for the same patients, depending on the MRI sequence used. These differences occur due to different variable sequence parameters such as slice thickness, different partial vol-

ume effects, and the relatively small sample size. Where measurements varied largely between cranial nerves VII and VIII, differences among the 4 used sequences were small. This result reflects the difficulty of comparing absolute morphometric parameters in the different MRI studies performed with different sequences on different scanners.¹⁹⁻²¹ Due to our small sample size, we calculated the intrarater and interrater correlation to make a statement about the reproducibility of our measurements. We found a very strong-to-strong positive

Table 3: Overview of the significant differences^a

Nerve	Parameters			P Values
	Measuring Point	Diameter or Area	Sequence	
VIII	CPA	CSA	FLAIR 0.3	.0098
VIII	CPA	SD	CISS 0.4	.0295
IVN	Meatus	CSA	CISS 0.6	.0021
IVN	Meatus	LD	CISS 0.6	.0229
FN	CPA	LD	CISS 0.4	.0208
FN	Meatus	LD	FLAIR 0.5	.0413
FN	Meatus	CSA	FLAIR 0.5	.0237
FN	Fundus	LD	CISS 0.4	.0033

^aThis table provides an overview of the significant differences of LD/SD and CSA without the Bonferroni correction ($P < .05$) of cranial nerve VIII, the IVN, and the FN at their different measuring points throughout their course from the CPA to the fundus of the IAC within the 4 used sequences (CISS 0.4, CISS 0.6, FLAIR 0.3, and FLAIR 0.5 sequences), obviously not following a specific pattern.

Table 4: Overview of nerve thickness as a function of the symptom duration^a

Nerve	Measuring Point	Parameter	Affected Side		Nonaffected Side	
			≤12 Months	≥120 Months	≤12 Months	≥120 Months
VIII	CPA	Mean	1.74 (SD, 0.46)	1.59 (SD, 0.39)	1.71 (SD, 0.44)	1.86 (SD, 0.43)
		P		.4032		.4218
CN	Meatus	Mean	0.40 (SD, 0.08)	0.37 (SD, 0.14)	0.43 (SD, 0.12)	0.39 (SD, 0.12)
		P		.4962		.4439
SVN	Meatus	Mean	0.34 (SD, 0.08)	0.32 (SD, 0.11)	0.32 (SD, 0.09)	0.31 (SD, 0.09)
		P		.6349		.7837
IVN	Meatus	Mean	0.30 (SD, 0.05)	0.28 (SD, 0.07)	0.31 (SD, 0.06)	0.29 (SD, 0.11)
		P		.5430		.6878
FN	CPA	Mean	0.45 (SD, 0.11)	0.35 (SD, 0.12)	0.41 (SD, 0.14)	0.38 (SD, 0.12)
		P		.0556		.6725
FN	Meatus	Mean	0.35 (SD, 0.09)	0.33 (SD, 0.17)	0.38 (SD, 0.11)	0.32 (SD, 0.19)
		P		.7656		.4096
FN	Fundus	Mean	0.36 (SD, 0.10)	0.32 (SD, 0.08)	0.38 (SD, 0.14)	0.33 (SD, 0.14)
		P		.3164		.4465

^aThis table shows the CSA areas (square millimeter) of cranial nerves VII (FN) and VIII and their branches (CN, SVN, and IVN) measured in the CPA or within the IAC (meatus and fundus) of the clinically unilaterally-affected patients with MD using the CISS 0.4 sequence and compares the 2 subgroups (symptom duration, maximum 12 versus minimum 120 months) by an independent samples *t* test (mean and *P*).

correlation, respectively, a very strong-to-moderate correlation, which means good reproducibility in trained examiners.

Study Limitations

Our study has several limitations. First, our sample size was limited, particularly for the subgroup analyses. Larger studies are warranted to confirm our results. Second, this time we did not compare our measurements with those of an age- and sex-matched healthy control cohort to analyze differences in a clinically unaffected control population. Only a few surveys¹⁹⁻²¹ with measurements of the cranial nerves VII and VIII have been published, mostly in normal-hearing patients. The comparison of these published data also showed differences of nerve diameters according to the measuring point and the MRI sequence used. Studies like ours encounter challenges related to measuring dimensions at the scale of fractions of millimeters. The ability to accurately discern small changes in diameter of this magnitude by volumetric MRI is limited, affecting the reliability and validity of the study results. We tried to minimize this limitation by measuring the LD and SD as well as the CSA on transverse sections with consistent windowing levels by the same 2 readers and were able to prove good reproducibility. Further and larger studies, including the repetition of the comparison with a healthy control group, are necessary to confirm our results. If possible, modern MRI techniques should be combined with histopathologic temporal bone investigations including photomicrographs of the inner ear and the vestibulocochlear nerve to get more insight into the pathophysiology of MD.

CONCLUSIONS

Our data showed no significant differences in diameters and CSAs of cranial nerves VII and VIII between the affected and the clinically nonaffected sides of unilaterally-affected patients with MD after Bonferroni correction for multiple testing. There was also no correlation to the duration of clinical symptoms. This finding may potentially point to a systemic process starting long before the onset of first clinical symptoms. Normative nerve diameters should only be used if comparable MRI sequence parameters are used because our data showed different means for the same patients at the same measuring points depending on the MRI sequences used. From our point of view, skipping additional strongly T2-weighted imaging, such as CISS sequences is feasible when endolymphatic hydrops imaging sequences are well-performed, because this choice reduces the examination time and enhances patient comfort.

Disclosure forms provided by the authors are available with the full text and PDF of this article at www.ajnr.org.

REFERENCES

1. Semaan MT, Alagramam KN, Megerian CA. **The basic science of Meniere's disease and endolymphatic hydrops.** *Curr Opin Otolaryngol Head Neck Surg* 2005;13:301-07 [CrossRef Medline](#)
2. Plontke SK, Gürkov R. **Menière's disease [in German].** *Laryngorhinootologie* 2015;94:530-54 [CrossRef Medline](#)
3. Berlinger NT. **Meniere's disease: new concepts, new treatments.** *Minn Med* 2011;94:33-36 [Medline](#)
4. Yang CH, Yang MY, Hwang CF, et al. **Functional and molecular markers for hearing loss and vertigo attacks in Meniere's disease.** *Int J Mol Sci* 2023;24:2504 [CrossRef Medline](#)
5. Tsuji K, Velazquez-Villasenor L, Rauch SD, et al. **Temporal bone studies of the human peripheral vestibular system. Meniere's disease.** *Ann Otol Rhinol Laryngol Suppl* 2000;181:26-31 [CrossRef Medline](#)
6. Kariya S, Cureoglu S, Fukushima H, et al. **Histopathologic changes of contralateral human temporal bone in unilateral Meniere's disease.** *Otol Neurotol* 2007;28:1063-68 [CrossRef Medline](#)
7. Megerian CA. **Diameter of the cochlear nerve in endolymphatic hydrops: implications for the etiology of hearing loss in Meniere's disease.** *Laryngoscope* 2005;115:1525-35 [CrossRef Medline](#)
8. Arweiler DJ, Jahnke K, Grosse-Wilde H. **Meniere disease as an autoimmune dominant hereditary disease [in German].** *Laryngorhinootologie* 1995;74:512-15 [CrossRef Medline](#)
9. Paparella MM, de Sousa LC, Mancini F. **Meniere's syndrome and otitis media.** *Laryngoscope* 1983;93:1408-15 [Medline](#)
10. Arenberg IK, Lemke C, Shambaugh GE Jr. **Viral theory for Ménière's disease and endolymphatic hydrops: overview and new therapeutic options for viral labyrinthitis.** *Ann N Y Acad Sci* 1997;830:306-13 [CrossRef Medline](#)
11. Vasama JP, Linthicum FH Jr. **Meniere's disease and endolymphatic hydrops without Meniere's symptoms: temporal bone histopathology.** *Acta Otolaryngol* 1999;119:297-301 [CrossRef Medline](#)
12. Gurkov R, Berman A, Dietrich O, et al. **MR volumetric assessment of endolymphatic hydrops.** *Eur Radiol* 2015;25:585-95 [CrossRef Medline](#)
13. Pyykko I, Nakashima T, Yoshida T, et al. **Meniere's disease: a reappraisal supported by a variable latency of symptoms and the MRI visualisation of endolymphatic hydrops.** *BMJ Open* 2013;3:e001555 [CrossRef](#)
14. Gurkov R, Flatz W, Ertl-Wagner B, et al. **Endolymphatic hydrops in the horizontal semicircular canal: a morphologic correlate for canal paresis in Meniere's disease.** *Laryngoscope* 2013;123:503-06 [CrossRef Medline](#)
15. Bernaerts A, Vanspauwen R, Blaivie C, et al. **The value of four stage vestibular hydrops grading and asymmetric perilymphatic enhancement in the diagnosis of Meniere's disease on MRI.** *Neuroradiology* 2019;61:421-29 [CrossRef Medline](#)
16. Paškonienė A, Baltagalvienė R, Lengvenis G, et al. **The importance of the temporal bone 3T MR imaging in the diagnosis of Meniere's disease.** *Otol Neurotol* 2020;41:235-41 [CrossRef Medline](#)
17. Deng W, Lin X, Su Y, et al. **Comparison between 3D-FLAIR and 3D-real IR MRI sequences with visual classification method in the imaging of endolymphatic hydrops in Meniere's disease.** *Am J Otolaryngol* 2022;43:103557 [CrossRef Medline](#)
18. Bernaerts A, Janssen N, Wuyts FL, et al. **Comparison between 3D SPACE FLAIR and 3D TSE FLAIR in Meniere's disease.** *Neuroradiology* 2022;64:1011-20 [CrossRef Medline](#)
19. Jaryszak EM, Patel NA, Camp M, et al. **Cochlear nerve diameter in normal hearing ears using high-resolution magnetic resonance imaging.** *Laryngoscope* 2009;119:2042-45 [CrossRef Medline](#)
20. Nakamichi R, Yamazaki M, Ikeda M, et al. **Establishing normal diameter range of the cochlear and facial nerves with 3D-CISS at 3T.** *Magn Reson Med* 2013;12:241-47 [CrossRef](#)
21. Kang WS, Hyun SM, Lim HK, et al. **Normative diameters and effects of aging on the cochlear and facial nerves in normal-hearing Korean ears using 3.0-Tesla magnetic resonance imaging.** *Laryngoscope* 2012;122:1109-14 [CrossRef Medline](#)
22. Henneberger A, Ertl-Wagner B, Reiser M, et al. **Morphometric evaluation of facial and vestibulocochlear nerves using magnetic resonance imaging: comparison of Meniere's disease ears with normal hearing ears.** *Eur Arch Otorhinolaryngol* 2017;274:3029-39 [CrossRef Medline](#)
23. Peng L, Xiao Y, Liu L, et al. **Evaluation of cochlear nerve diameter and cross-sectional area in ANSD patients by 3.0-Tesla MRI.** *Acta Otolaryngol* 2016;136:792-99 [CrossRef Medline](#)

24. Tyrrell JS, Whinney DJ, Ukoumunne OC, et al. **Prevalence, associated factors, and comorbid conditions for Ménière's disease.** *Ear Hear* 2014;35:e162–69 [CrossRef Medline](#)
25. Liu Y, Jia H, Shi J, et al. **Endolymphatic hydrops detected by 3-dimensional fluid-attenuated inversion recovery MRI following intratympanic injection of gadolinium in the asymptomatic contralateral ears of patients with unilateral Ménière's disease.** *Med Sci Monit* 2015;21:701–07 [CrossRef Medline](#)
26. Ark ED, Boya MN, Shah A, et al. **Four-hour-delayed gadolinium 3D REAL IR and SPACE FLAIR MRI correlated to Meniere disease histology.** *Ear Nose Throat J* 2024 Jun 13 [Epub ahead of print] [CrossRef Medline](#)
27. **Committee on Hearing and Equilibrium Guidelines for the diagnosis and evaluation of therapy in Meniere's disease: American Academy of Otolaryngology-Head and Neck Foundation, Inc.** *Otolaryngol-Head and Neck Surg* 1995;113:181–85 [CrossRef Medline](#)
28. Gurkov R, Kantner C, Strupp M, et al. **Endolymphatic hydrops in patients with vestibular migraine and auditory symptoms.** *Eur Arch Otorhinolaryngol* 2014;271:2661–67 [CrossRef Medline](#)
29. Gurkov R, Pytko I, Zou J, et al. **What is Meniere's disease? A contemporary re-evaluation of endolymphatic hydrops.** *J Neurol* 2016;263(Suppl 1):S71–81 [CrossRef Medline](#)
30. Nakashima T, Pytko I, Arroll MA, et al. **Meniere's disease.** *Nat Rev Dis Primers* 2016;2:16028 [CrossRef Medline](#)
31. Shi S, Guo P, Li W, et al. **Clinical features and endolymphatic hydrops in patients with MRI evidence of hydrops.** *Ann Otol Rhinol Laryngol* 2019;128:286–92 [CrossRef Medline](#)
32. Jerin C, Krause E, Ertl-Wagner B, et al. **Longitudinal assessment of endolymphatic hydrops with contrast-enhanced magnetic resonance imaging of the labyrinth.** *Otol Neurotol* 2014;35:880–83 [CrossRef Medline](#)
33. Nakashima T, Naganawa S, Katayama N, et al. **Clinical significance of endolymphatic imaging after intratympanic gadolinium injection.** *Acta Otolaryngol Suppl* 2009(560):9–14 [CrossRef Medline](#)
34. Nakashima T, Naganawa S, Sugiura M, et al. **Visualization of endolymphatic hydrops in patients with Meniere's disease.** *Laryngoscope* 2007;117:415–20 [CrossRef Medline](#)
35. Barath K, Schuknecht B, Naldi AM, et al. **Detection and grading of endolymphatic hydrops in Meniere disease using MR imaging.** *AJNR Am J Neuroradiol* 2014;35:1387–92 [CrossRef Medline](#)
36. Neri G, Tartaro A, Neri L. **MRI with intratympanic gadolinium: comparison between otoneurological and radiological investigation in Ménière's disease.** *Front Surg* 2021;8:672284 [CrossRef Medline](#)
37. Diorflar S, Guigou C, Daguët E, et al. **Confrontation of endolymphatic hydrops diagnosis on 3-Tesla MRI to clinical and audiovestibular findings in Meniere's disease.** *Front Neurol* 2023;14:1105461 [CrossRef Medline](#)
38. Paparella MM, Djalilian HR. **Etiology, pathophysiology of symptoms, and pathogenesis of Meniere's disease.** *Otolaryngol Clin North Am* 2002;35:529–45, vi [CrossRef Medline](#)
39. Liu Y, Yang J, Duan M. **Current status on researches of Meniere's disease: a review.** *Acta Otolaryngol* 2020;140:808–12 [CrossRef Medline](#)
40. Arbusow V, Derfuss T, Held K, et al. **Latency of herpes simplex virus type-1 in human geniculate and vestibular ganglia is associated with infiltration of CD8+ T cells.** *J Med Virol* 2010;82:1917–20 [CrossRef Medline](#)
41. Xu W, Li X, Song Y, et al. **Ménière's disease and allergy: epidemiology, pathogenesis, and therapy.** *Clin Exp Med* 2023;23:3361–71 [CrossRef Medline](#)
42. Xie S, Zhang R, Tang Y, et al. **Exploring causal correlations between inflammatory cytokines and Ménière's disease: a Mendelian randomization.** *Front Immunol* 2024;15:1373723 [CrossRef Medline](#)
43. Frejo L, Lopez-Escamez JA. **Cytokines and inflammation in Meniere disease.** *Clin Exp Otorhinolaryngol* 2022;15:49–59 [CrossRef Medline](#)
44. Klockars T, Kentala E. **Inheritance of Meniere's disease in the Finnish population.** *Arch Otolaryngol Head Neck Surg* 2007;133:73–77 [CrossRef Medline](#)
45. Mohseni-Dargah M, Falahati Z, Pastras C, et al. **Meniere's disease: pathogenesis, treatments, and emerging approaches for an idiopathic bioenvironmental disorder.** *Environ Res* 2023;238:116972 [CrossRef Medline](#)
46. Hess A, Bloch W, Huverstuhl J, et al. **Expression of inducible nitric oxide synthase (iNOS/NOS II) in the cochlea of guinea pigs after intratympanic endotoxin-treatment.** *Brain Res* 1999;830:113–22 [CrossRef Medline](#)
47. Kong WJ, Ren T, Nuttall AL. **Electrophysiological and morphological evaluation of the acute ototoxicity of sodium nitroprusside.** *Hear Res* 1996;99:22–30 [CrossRef Medline](#)
48. Ishiyama G, Lopez IA, Sepahdari AR, et al. **Meniere's disease: histopathology, cytochemistry, and imaging.** *Ann N Y Acad Sci* 2015;1343:49–57 [CrossRef Medline](#)
49. Lopez-Escamez JA, Liu Y. **Epidemiology and genetics of Meniere's disease.** *Curr Opin Neurol* 2024;37:88–94 [CrossRef Medline](#)
50. Yuan X, Li X, Xu Y, et al. **Microstructural changes of the vestibulocochlear nerve in patients with Ménière's disease using diffusion tensor imaging.** *Front Neurol* 2022;13:915826 [CrossRef Medline](#)